LIMNOLOGY
and
OCEANOGRAPHY: METHODS

ASLO

*Limnol. Oceanogr.: Methods* 14, 2016, 759–766

doi: 10.1002/lom3.10136

# μCT scanning—a novel method for in vivo 3D characterization of zooplankton propagules

**Tom Pinceel,*[1] Enya Wynants,[1] Nathalie Tonné,[2] Luc Brendonck,[1] Bram Vanschoenwinkel[2]**
[1]Laboratory of Aquatic Ecology, Evolution and Conservation, KU Leuven, Leuven, Belgium
[2]Ecology and Biodiversity section, Department of Biology, Vrije Universiteit Brussel (VUB), Brussels, Belgium

## *Abstract*

Many zooplankton species produce dormant stages to bridge episodes that are unfavorable for juveniles and adults. Although a variety of methods has been used to study the morphology and internal structure of these propagules, surprisingly little is known about links between propagule traits and life history characteristics such as dormancy, hatching behavior and fitness of emerging larvae. A major constraint is that most available methods are lethal to the embryo and processing can generate visual artefacts. Here, we investigate the potential of High Resolution X-ray Computed Tomography (HRXCT or μCT scanning) to compile whole mount 3D reconstructions of the propagules of three zooplankton species that differ in size (∼200–1200 $\mu$m) and shape (spherical eggs vs. semi-circular ephippia). Our results show that μCT scanning is a suitable technique for whole mount reconstruction of propagules. In addition, by combining the scanning procedure with a laboratory hatching experiment we showed that while eggs that were exposed to μCT scanning had significantly lower hatching fractions and lower motility of hatchlings than control eggs, some of the scanned eggs or larvae could still be used in subsequent life table experiments. Overall, μCT scanning represents a valuable, non-invasive technique for internal and external characterization of zooplankton propagules and to study associations between propagule structure and life history traits.

To bridge episodes of unfavorable growing conditions, many zooplankton species produce resistant, dormant stages that are added to a persistent propagule bank in the sediment from which a new active population can be recruited when suitable conditions return (Gyllström and Hansson 2004). Besides allowing zooplankton to disperse through time via dormancy, dormant stages (hereinafter referred to as "propagules") can also be picked-up and carried to other habitats by vectors such as water, wind and animals, thereby resulting in spatial dispersal (Bilton et al. 2001). The observation of extensive intra- and interspecific trait variation among propagules has sparked the formulation of many hypotheses that try to explain the adaptive significance of specific structures. These include anti-predator defence (Cáceres and Hairston 1998; Dumont et al. 2002), promotion of chemical exchange (Belmonte et al. 1997), optimal packing of resting eggs in brood pouches (Brendonck et al. 1992) and inhibition as well as facilitation of dispersal via vectors such as wind, water and animals (Brendonck et al. 1992; Figuerola and Green 2002; Brochet et al. 2010; Pinceel et al. 2016). Similarly, observations of variation in species trait values such as hatching behavior, dispersal propensity and maturation time have stimulated researchers to look for propagule traits that may offer a mechanistic explanation for these observed differences (Pietrzak and Slusarczyk 2006; Pinceel et al. 2013*a*,*b*).

Nonetheless, empirical studies that have succeeded to actually demonstrate a mechanistic link between internal or external morphological variation in propagules and specific life history traits and responses in subsequent active life stages are largely deficient. This knowledge gap can mostly be attributed to a number of practical challenges that constrain the morphological and anatomical characterization of zooplankton propagules. First of all, they are typically very small (∼50–1500 $\mu$m) (Brendonck and De Meester 2003) and the study of specific substructures therefore requires high level magnification. Second, dormant embryos are generally surrounded by a non-transparent egg shell or envelope. This limits the potential of observation techniques that rely on transillumination, such as classic bright field microscopy, where an image is composed by capturing light that has

Additional Supporting Information may be found in the online version of this article.

*Correspondence: tom.pinceel@bio.kuleuven.be

been transmitted through a sample. In previous zooplankton studies, Scanning Electron Microscopy (SEM) has been most commonly used to obtain high resolution two dimensional (2D) images of propagules (e.g., Gilchrist 1978; Brendonck and Coomans 1994; Brendonck and Riddoch 1997; Timms and Lindsay 2011; Pinceel et al. 2013a, 2015). However, this technique is "destructive" since it requires gold-sputter coating. In addition, only surface structures can be visualized through SEM. To investigate internal propagule structures, the specimen needs to be submerged in liquid nitrogen and subsequently cut in subsections. The preparation process and physical cutting are time consuming and likely to disrupt the original structure and introduce imaging artefacts which complicate interpretation (Al-Amoudi et al. 2005; Weston et al. 2010).

The most comprehensive way to characterize zooplankton propagules would be to build and subsequently analyse three dimensional (3D) reconstructions in which both internal and external structures can be studied. This can, for instance, be achieved by making a large number of cross sections, subject these to SEM or bright field microscopy and combine the images. That is, however, a time consuming and costly procedure. Furthermore, specimens are destroyed to make the sections and this approach, therefore, does not enable in vivo analyses. Alternatively, 3D reconstructions can be automated in a, so-called, whole mount study. Existing techniques that have been most commonly used for visualising animal and plant tissues in whole mount studies include Micro Magnetic Resonance Imaging (μMRI), Optical Projection Tomography (OPT) and High Resolution X-ray Computed Tomography (HRXCT or μCT scanning) (Staedler et al. 2013). Since the resolution of μMRI is limited (~25–50 $\mu$m) (Rengle et al. 2009), it is not suited for accurate 3D imaging of most zooplankton propagules because of their small size. Although the resolution of OPT is much higher (~1.5–3 $\mu$m), it requires samples to be transparent since it is a transillumination technique. This implies that zooplankton propagules should be treated with a clearing agent, such as NaOH, prior to visualization (Staedler et al. 2013). Therefore, the technique would be lethal or influence dormant embryos in another way and is not suitable for in vivo imaging followed by life history experiments. A more promising method is HRXCT (hereinafter referred to as "μCT scanning"). First developed in the 1970s for medical applications, this technique has been optimized for the study of microscopic plant structures including wood, roots and seeds (Steppe et al. 2004; Cloetens et al. 2006; Dhondt et al. 2010; Staedler et al. 2013; Yamauchi et al. 2013) but also small animal imaging (Metscher 2009; Schambach et al. 2010). μCT scanning can generally be performed without sample preparation with a resolution of up to ~0.4 $\mu$m. The scanning procedure has been shown to be non-lethal and non-destructive for living animal (Hagenmüller et al. 2007) and plant (Ferreira et al. 2010) cells. Nonetheless, X-rays are known to have an ionizing effect (Zhou et al. 2006) and have, for instance, been shown to partly inhibit growth of rockcress (*Arabidopsis* spp.) seedlings after repeated exposure (Dhondt et al. 2010).

In this study, we investigated whether μCT scanning can be used as an in vivo observation technique in whole mount reconstructions of zooplankton propagules. For this, we selected three zooplankton model species; *Branchipodopsis wolfi* Daday 1910, *Triops cancriformis* Bosc 1801 and *Daphnia magna* Straus 1820. We specifically selected these species since they produce propagules of different sizes and shapes. While *B. wolfi* and *T. cancriformis* both produce spherical eggs with a typical diameter of ~190 $\mu$m and ~390 $\mu$m, respectively, the water flea *D. magna* produces resting eggs that are encased pairwise in a semi-circular envelope with a typical total size along the longest axis of ~1180 $\mu$m (Pinceel et al. 2016). In order to investigate whether embryos could still be used in life table experiments after being scanned, we assessed the hatching fraction of exposed eggs and the motility of emerged larvae of the model species *B. wolfi*.

## Materials and procedures

### Study organisms

Three zooplankton species were selected from three different orders of branchiopod crustaceans (Crustacea, Branchiopoda). The selection included; dormant eggs of the fairy shrimp *B. wolfi* (Anostraca) (Fig. 1a) and the tadpole shrimp *T. cancriformis* (Notostraca) (Fig. 1b) and ephippia of the water flea *D. magna* (Cladocera) (Fig. 1c). Populations of all branchiopod species were reared for at least two generations under standardized laboratory conditions before their eggs were collected for these experiments. The *B. wolfi* laboratory population originated from a mixed sample of six temporary rock pool populations from Korannaberg in South Africa, the *T. cancriformis* population from a wetland in the Camargue region in France and the *D. magna population* from a commercial breeding facility (Microbiotests, Gent, Belgium). Prior to experimentation, propagules were dried in transparent polystyrene petri-dishes for 8 weeks in a temperature controlled incubator at 18°C (relative humidity air: 78%) and a 12 h light/dark cycle. Both *B. wolfi* and *T. cancriformis* are restricted to temporary waters and their eggs generally require dehydration to ensure optimal dormancy release and hatching (Dumont and Negrea 2002; Vanschoenwinkel et al. 2010). By using the propagules of these three different species, we were able to perform a first evaluation of μCT scanning for 3D imaging of zooplankton propagules of different size (~200–1200 $\mu$m) and shape (spherical eggs vs. semi-circular ephippia holding two eggs). In addition, the propagules of the three selected species differ in external ornamentation. While *T. cancriformis* and *D. magna* propagules have a more or less smooth outer surface, the *B. wolfi* egg-surface is characterized by ridges. Furthermore, *D. magna* ephippia have antler-like outgrowths with small hooks on their

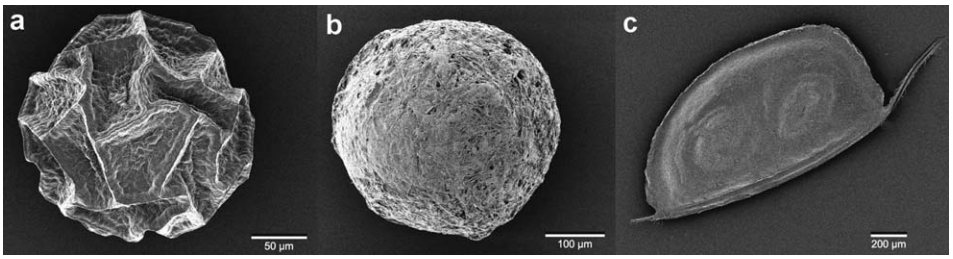


**Fig. 1.** Scanning Electron Microscopy produces high resolution images of the propagules of the three investigated species; (**a**) the fairy shrimp *B. wolfi*, (**b**) the tadpole shrimp *T. cancriformis* and (**c**) the water flea *D. magna*.

surface (Pinceel et al. 2016). By including variation in surface structures among the investigated propagules, we could assess the limits of μCT scanning for visualising small surface projections.

### μCT procedure

μCT scanning was performed on whole zooplankton propagules using a SkyScan 1172 (Bruker, Kontich, Belgium). During the scanning process, objects are illuminated by a microfocus X-ray source and a planar X-ray detector collects magnified projection images. Since the object rotates, hundreds of views are acquired which can be computer-synthesized into a stack of virtual cross section slices through the object. All specimens were scanned at the μCT scanning facilities at the Vrije Universiteit Brussel (Belgium). Total costs amounted to ~10.45 USD scanning-$h^{-1}$.

Scans were performed on whole and viable propagules without any sample preparation. Prior to the scanning procedure, propagules of all three species were positioned on a metal stub and spaced at least 2000 $\mu$m apart. Four stubs were prepared each holding 1 *T. cancriformis* egg, 2 *B. wolfi* eggs, and 1 *D. magna* ephippium. A camera binning mode of 1 by 1 pixels (maximum resolution) was used, resulting in projection images of 4000 by 2664 pixels. An isotropic pixel resolution of 0.73 $\mu$m was obtained. No filter was used, and scanning was operated at 31 kV and 181 $\mu$A for approximately 10 h. This relatively low X-ray energy level is particularly suited for scanning biological samples (Verboven et al. 2013). Projection images were taken with a rotation step of 0.2° over 360°, exposure times were set to 2470 ms and the signal to noise ratio of the projection images was improved by using a frame averaging of 6 for every exposure. We ran a second scanning protocol to investigate whether high-quality images could also be obtained during only 3 h of scanning by reducing the acquisition arc to 180° and operating at 35 kV and 211 $\mu$A. For this scan, exposure times were set to 1750 ms using a frame averaging of 4. Propagules were exposed to a radiation dose of ~1.5 and ~2.2 kGy scanning-$h^{-1}$ with the first and second scanning protocol, respectively (as estimated with the "Rad Pro Calculator tool"; McGinnis 2009). During the scanning process, temperatures of ~30°C were reached in the scanner.

While the scanning times were relatively high in this study, this should not be a major constraint for the application of the technique. After all, a large number of propagules can be scanned simultaneously and, after having been initiated, the scanning process is entirely self-operating.

Slice-reconstructions were performed with the NRecon v1.6.2.0 software according to cone-beam algorithms with automated adaptation to the specific scanning geometry of the scanner. Individual eggs were selected as separate regions of interest with the CTAn v1.15 package. Sets of slices were subsequently combined into 3D reconstructions of each propagule with the CTVox v3.1.1 package. Images were exported in JPG format. All software packages were produced by Bruker (Kontich, Belgium).

### The impact of μCT scanning on hatching behavior and motility

In the second part of this study, we investigated whether μCT scanning influences the hatching behavior of zooplankton propagules and the motility of newly emerged larvae. To assess this, we randomly subdivided a batch of 200 intact *B. wolfi* eggs in two groups of 100 eggs and subjected one group to μCT scanning while the second group served as a control. The control eggs underwent identical manipulations to the exposed group with the exception of being scanned.

Subsequently, we conducted a common garden laboratory hatching experiment to look for differences in hatching fraction between exposed and unexposed eggs. Each of the 200 eggs was positioned individually in a well of a transparent polystyrene multi-well plate (6 × 4 wells). Eggs were randomized over well plates by randomly assigning either eggs from the exposed- or from the control condition to each row of six wells. To account for the influence of "row identity," we included it as a random blocking factor in the statistical analyses. At the start of an inundation, each well was filled with 2 mL of Environmental Protection Agency (EPA) medium with a conductivity of 50 $\mu$s $cm^{-1}$ (distilled water with 0.00033 mol $L^{-1}$ $NaHCO_3$, 0.000098 mol $L^{-1}$ $CaSO_4.2H_2O$, 0.00014 mol $L^{-1}$ $MgSO_4$, 0.000015 mol $L^{-1}$ KCl; Anonymous 1985). All plates were randomly positioned in a temperature controlled incubator at 18°C under continuous light (full spectrum, 4000 lux, lamp type Osram L 8W/640; Osram,

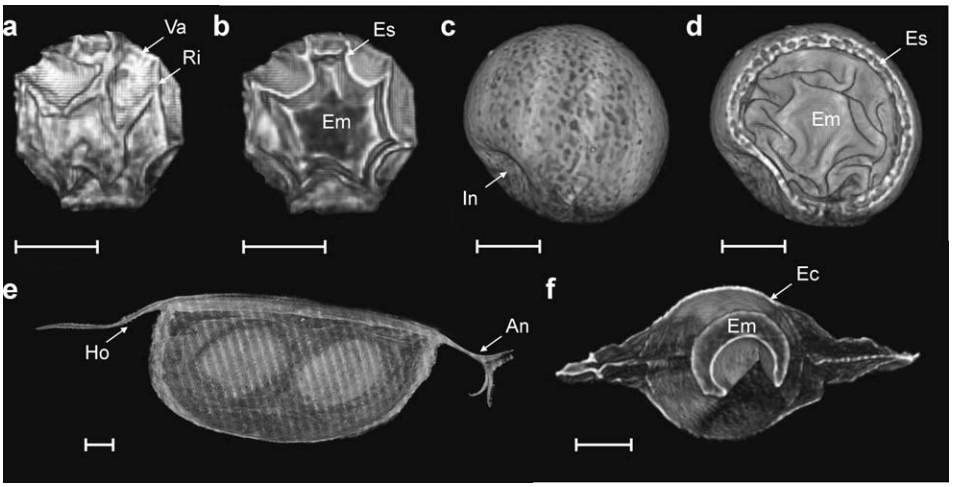


**Fig. 2.** μCT scanning images for whole mount reconstructions of zooplankton resting stages of different sizes and types; (**a**) complete and (**b**) cross-section image of a *B. wolfi* dormant egg, (**c**) complete and (**d**) cross-section image of a *T. cancriformis* dormant egg and (**e**) complete and (**f**) lateral section image of a *D. magna* ephippium. All scale bars indicate 100 μm. A number of morphological traits were marked on the images; antler like appendage (An), ephippial capsule (Ec), embryo (Em), egg shell (Es), hook structure (Ho), invagination (In), ridge (Ri), and valley (Va).

Rotterdam, The Netherlands). These inundation conditions correspond to optimal laboratory hatching conditions for the investigated *B. wolfi* population (Vanschoenwinkel et al. 2010). Hatching was evaluated at 12 h intervals until no new hatchlings were observed for 32 h. Plates were randomly repositioned in the incubator after each evaluation of hatching.

### Statistical analyses

The impact of μCT scanning on hatching was investigated using a Generalised Linear Mixed Model (GLMM) specifying a binomial error distribution and corresponding *logit* link function since hatching was measured as a 0/1 response of individual eggs. In this model, "row identity" was included as a random factor and μCT scanning as a fixed categorical predictor. In addition, we built a second GLMM to investigate the effect of μCT scanning as a fixed categorical predictor on the motility of newly hatched nauplius larvae. "Row identity" was included as a random factor in this model and only hatched eggs were considered. Motility was scored as a 0/1 response since larvae were either swimming or inactive. Given that the most likely effect of X-rays on hatching of eggs or motility of hatchlings would be negative, it is sensible to perform one-sided tests that assess negative effects of the treatment on both responses. All analyses were performed in R (version 3.1.1; R Core Development Team) with the packages car (companion to applied regression), stats (statistical calculations and random number generation) and lme4 (linear mixed-effects models).

## Assessment

μCT scanning followed by 2D slide- and 3D geometric reconstructions generated high quality images of whole zooplankton propagules with clear visibility of external and internal structures (Fig. 2b, d, f; see also Supporting Information (SI) 1 for additional images). Embryonic tissue is distinguishable from outer membranes and cavities in all of the three investigated species. However, no substructures are visible within the embryonic tissue.

Images of *B. wolfi* eggs are of the lowest quality. The results suggest an empty space between the embryo and the egg shell. Yet, the shape of the embryo is adapted to the curves of the egg shell (Fig. 2b; Supporting Information Fig. 1). Within the *T. cancriformis* eggs, only about two-thirds of the internal space is occupied by the embryo whereas the rest is an empty cavity. Although *T. cancriformis* eggs are spherical, the embryo is folded and has several invaginations. Within the egg shell, cavities could be observed (Fig. 2c,d; Supporting Information Fig. 2). Finally, the images of the *D. magna* propagules show that the ephippium is composed of several separate layers with air cavities. Furthermore, it shows the embryo is in a bended position. The antler-like appendages at the extremities of the ephippium are clearly visible (Fig. 2e,f; Supporting Information Fig. 3).

Hatching fractions were lower for scanned *B. wolfi* eggs (28%) than for control group eggs (40%) ($Z_{36,\ 35} = -1.847$, $p = 0.065$, $p_{\text{one sided}} = 0.0325$, Estimate = −0.564) (Fig. 3). The second GLMM demonstrated a significant negative effect of scanning on the motility of hatched larvae ($Z_{30,\ 29} = -2.055$, $p = 0.040$, $p_{\text{one sided}} = 0.020$, Estimate = −1.153). Whereas only 22% of the larvae that emerged from exposed eggs was motile, motility was 48% in the control group.

## Discussion

Zooplankton propagules are typically small with non-transparent outer layers. This complicates detailed imaging and impedes the study of internal structures in a non-invasive way via standard transillumination methods. Our

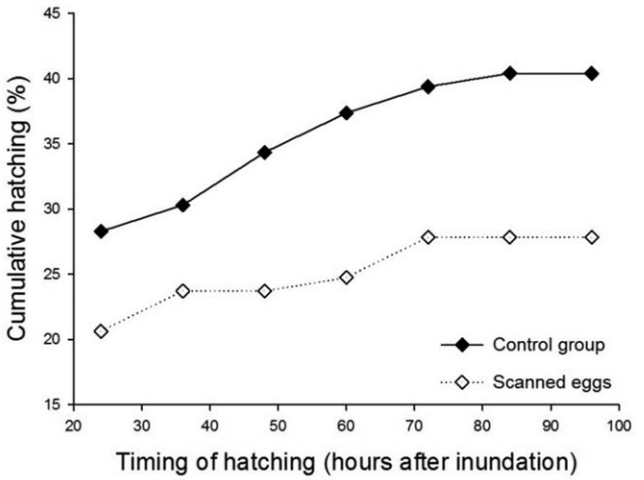


**Fig. 3.** The impact of μCT scanning on the hatching behavior of *B. wolfi* resting eggs. The hatching fraction of eggs that were exposed to the scanning procedure was reduced compared to the hatching fraction of the control group of eggs.

findings demonstrate that μCT scanning is a useful technique in non-invasive whole mount imaging. Although scanning impacted the viability of dormant zooplankton embryos (i.e., hatching of eggs and motility of emerged larvae), at least some of the scanned eggs or larvae could still be used in subsequent life table experiments. Therefore, μCT scanning could be useful for integrated studies that attempt to directly link the morphology of zooplankton propagules to subsequent life history responses and trait values.

μCT scanning generated detailed and complete 3D images of the propagules of the three investigated species on which traits such as egg size, embryo size and position within the egg, egg shell thickness and the size and position of cavities can be measured. Although the pixel-size of the generated images in our study was 0.73 $\mu$m, the true spatial resolution (because of the 10% modulation transfer function) of the scans was $\sim 4$ $\mu$m. Still, because of small angle scattering, smaller details could be observed at the focal spot. The μCT scanning resolution is about two to three orders of magnitude lower than that of SEM pictures (Staedler et al. 2013). Whereas this resolution is sufficiently high to, for instance, analyse the small hooks that are present on the antler-like appendages of the relatively large ($\sim 1200$ $\mu$m) *D. magna* ephippia, it is insufficient to study structures such as the micro-pores ($< 1$ $\mu$m) in the outer egg shell of the small ($\sim 200$ $\mu$m) *B. wolfi* eggs. The latter can be visualized through SEM (Pinceel et al. 2013a). Recently, so-called nanoCT scanners have been developed (e.g., SkyScan 2011; Bruker, Kontich, Belgium) with an improved, sub-micron, spatial resolution. Such scanners could serve to generate images of whole zooplankton propagules with a maximum size of up to 1000 $\mu$m at this maximum resolution. Yet, only a very limited number of these devices are currently available which could, at the moment, constrain the general use of the technique.

It must be noted that no substructures could be detected in the embryos of any of the three investigated species. Although μCT scanning generally provides good spatial resolution, "soft tissue contrast" is often poor (Schambach et al. 2010). Therefore, the method is most likely unsuitable for detailed studies of the embryo. Staining with contrast agents such as osmium tetroxide and phosphomolybdic acid could improve the visibility of embryonic substructures. Yet, treatment with such agents would most likely be harmful to the embryo (Metscher 2009; Descamps et al. 2014) and since we were exploring the potential of μCT scanning as an in vivo technique, we chose not to use staining in this first study.

Although μCT scanning is non-invasive and considered minimally destructive (Hagenmüller et al. 2007; Ferreira et al. 2010), samples are exposed to a high dose of X-rays during the scanning process, which can have harmful ionising effects by dislodging electrons from atoms (Zhou et al. 2006). The developing ions, in turn, can engage in chemical reactions with other molecules. This can result in disruption of biochemical pathways, cell death and mutagenesis (Parashar et al. 2008; Dhondt et al. 2010; Beltrán-Pardo et al. 2013). Within our study, propagules were exposed to a radiation dose of ~1–2 kGy scanning-h$^{-1}$. Although this is a high radiation dose, it does not necessarily mean that propagules effectively absorbed such a dose since absorption is dependent on traits including the propagule structure, size and density. Yet, we did observe significantly lower hatching in *B. wolfi* eggs that were subjected to scanning compared to unexposed eggs. Quantitatively, hatching fractions dropped from 40% to 28%. In absolute terms this is a reduction of 12% or 30%, depending on whether it is calculated based on the measured fractions (−12%) or relative to the percentage that hatched in the control treatment (−30%). Significantly fewer hatchlings from scanned eggs (22%) were actively swimming compared to hatchlings from eggs that were kept under control conditions (48%). Even under control conditions there was no complete hatching with only a fraction of the *B. wolfi* eggs hatching (40%). However, this was consistent with our expectations since the studied *B. wolfi* populations originate from rain-fed temporary rock pool habitats with highly variable flooding events, located on Korannaberg in South Africa (Tuytens et al. 2014). In these habitats, *B. wolfi* eggs are typically characterized by partial hatching which could represent a bet hedging strategy that divides their offspring over several inundations to buffer against unpredictable reproductive catastrophes (Brendonck and Riddoch 2000; Pinceel et al. 2013a). Overall, our results suggest that μCT scanning has a negative effect on the hatching and motility of zooplankton individuals that were exposed as dehydrated, dormant embryos. In order to minimize these harmful effects, resolution could be sacrificed or samples could be scanned only partially (e.g., rotation over 180°

instead of 360° as in the second scanning configuration provided in the "Materials and procedures" section) at the benefit of reduced exposure or if the required image-resolution is low. The fact that part of the *B. wolfi* embryos did survive exposure to high radiation doses in this study implies that they are highly resistant to the ionising effects of X-rays. Analogous to tardigrade dormant stages, which are known to be resistant to large doses of ionizing radiation, the high resistance of zooplankton eggs is most likely a by-product of the adaptations that evolved to allow their survival under extreme conditions including drought and UV exposure (Brendonck and De Meester 2003; Jönsson 2003). There could, however, be more severe negative effects that only become apparent during later life stages and were not investigated in this study. Also, it remains to be assessed whether the resilience of exposed propagules to μCT scanning is dependent on their developmental stage. After all, studies on the harmful effects of ionizing radiation on dormant embryos of other invertebrates, such as tardigrades, have shown that their sensitivity depends on the developmental stage during which they are exposed (Beltrán-Pardo et al. 2013).

## Comments and recommendations

μCT scanning could represent a valuable technique for detailed in vivo whole mount studies of zooplankton propagules. Whereas techniques such as SEM can generate higher resolution images, which is especially valuable for the study of small propagules and micro structures, μCT scanning holds several advantages. First of all, μCT scanning can generate high quality images of whole propagules without any sample preparation. Not only does this reduce the workload (and potential costs) involved with morphological studies of propagules, it also prevents the introduction of shearing and other physical artefacts that are linked to slicing samples. Second, at least some dormant zooplankton embryos survive μCT scanning and are characterized by a normal hatching and motility response afterwards. This means that μCT scanning could serve as a tool for in vivo characterization of propagule and embryo traits, which could subsequently be linked to life history trait values and responses in laboratory experiments. Finally, because of the virtual 3D reconstructions and flexible work-space, researchers are able to "navigate" through investigated propagules and conduct real-time morphological, anatomical and volumetric analyses.

## References

Al-Amoudi, A., D. Studer, and J. Dubochet. 2005. Cutting artefacts and cutting process in vitreous sections for cryo-electron microscopy. J. Struct. Biol. **150**: 109–121. doi: 10.1016/j.jsb.2005.01.003

Anonymous. 1985. Methods for measuring the acute toxicity of effluents to freshwater and marine organisms. US Environmental Protection Agency Report EPA/600/604-685/013.

Belmonte, G., A. Miglietta, F. Rubino, and F. Boero. 1997. Morphological convergence of resting stages of planktonic organisms: A review. Hydrobiologia **355**: 159–165. Doi: 10.1023/A:1003071205424

Beltrán-Pardo, E., K. I. Jönsson, A. Wojcik, S. Haghdoost, and M. Harms-Ringdahl. 2013. Effects of ionizing radiation on embryos of the tardigrade milnesium cf. tardigradum at different stages of development. PloS one **8**: e72098. doi: 10.1371/journal.pone.0072098

Bilton, D. T., J. R. Freeland, and B. Okamura. 2001. Dispersal in freshwater invertebrates. Annu. Rev. Ecol. Syst. **32**: 159–181. Doi:10.1146/annurev.ecolsys.32.081501.114016

Brendonck, L., M. L. Hamer, and A. Thiery. 1992. Occurrences of tetrahedral eggs in the Streptocephalidae Dady (Branchiopoda: Anostraca) with descriptions of a new subgenus, Parastreptocephalus, and a new species Streptocephalus (Parastreptocephalus) zuluensis Brendonck and Hamer. J. Crustacean Biol. **12**: 282–297. doi:10.2307/1549081

Brendonck, L., and A. Coomans. 1994. Egg morphology in African Streptocephalidae (Crustacea: Branchiopoda: Anostraca) Part 1: South of Zambezi and Kunene rivers. Arch. Hydrobiol. Suppl. **99**: 313–334.

Brendonck, L., and B. J. Riddoch. 1997. Anostracans (Branchiopoda) of Botswana: Morphology, distribution, diversity, and endemicity. J. Crustacean Biol. **17**: 111–134. doi: 10.1163/193724097X00151

Brendonck, L., and B. J. Riddoch. 2000. Egg bank dynamics in Anostracan desert rock pool populations (Crustacea: Branchiopoda). Arch. Hydrobiol. **148**: 71–84.

Brendonck, L., and L. De Meester. 2003. Egg banks in freshwater zooplankton: Evolutionary and ecological archives in the sediment. Hydrobiologia **491**: 65–84. doi:10.1023/A:1024454905119

Brochet, A. L., M. Gauthier-Clerc, M. Guillemain, H. Fritz, A. Waterkeyn, A. Baltanás, and A. J. Green. 2010. Field evidence of dispersal of branchiopods, ostracods and bryozoans by teal (Anas crecca) in the Camargue (southern France). Hydrobiologia **637**: 255–261. doi:10.1007/s10750-009-9975-6

Cáceres, C. E., and N. G. Hairston. 1998. Benthic-pelagic coupling in planktonic crustaceans: The role of the benthos. Adv. Limnol. **52**: 163–174. doi:10.1007/s003000050269

Cloetens, P., R. Mache, M. Schlenker, and S. Lerbs-Mache. 2006. Quantitative phase tomography of Arabidopsis seeds reveals intercellular void network. Proc. Natl. Acad. Sci. USA **103**: 14626–14630. doi:10.1073/pnas.0603490103

Descamps, E., A. Sochacka, B. De Kegel, D. Van Loo, L. Van Hoorebeke and D. Adriaens. 2014. Soft tissue

discrimination with contrast agents using micro-CT scanning. Belg J Zool. **144**: 20–40.

Dhondt, S., H. Vanhaeren, D. Van Loo, V. Cnudde, and D. Inzé. 2010. Plant structure visualization by high-resolution X-ray computed tomography. Trends Plant Sci. **15**: 419–422. doi:10.1016/j.tplants.2010.05.002

Dumont, H. J., S. Nandini, and S. S. S. Sarma. 2002. Cyst ornamentation in aquatic invertebrates: A defence against egg-predation. Hydrobiologia **486**: 161–167. doi:10.1023/A:1021346601235

Dumont, H. J., and S. V. Negrea. 2002. Introduction to the class Branchiopoda. Backhuys Publishers.

Ferreira, S. J., M. Senning, S. Sonnewald, P. M. Keßling, R. Goldstein, and U. Sonnewald. 2010. Comparative transcriptome analysis coupled to X-ray CT reveals sucrose supply and growth velocity as major determinants of potato tuber starch biosynthesis. BMC Genomics **11**: 93. doi:10.1186/1471-2164-11-93.

Figuerola, J., and A. J. Green. 2002. Dispersal of aquatic organisms by waterbirds: A review of past research and priorities for future studies. Freshw. Biol. **47**: 483–494. doi:10.1046/j.1365-2427.2002.00829.x

Gilchrist, B. M. 1978. Scanning electron microscope studies of the egg shell in some Anostraca (Crustacea: Branchiopoda). Cell Tissue Res. **193**: 337–351. doi:10.1007/BF00209045

Gyllström, M., and L. A. Hansson. 2004. Dormancy in freshwater zooplankton: Induction, termination and the importance of benthic-pelagic coupling. Aquat. Sci. **66**: 274–295. doi:10.1007/s00027-004-0712-y

Hagenmüller, H., S. Hofmann, T. Kohler, H. P. Merkle, D. L. Kaplan, G. Vunjak-Novakovic, R. Müller, and L. Meinel. 2007. Non-invasive time-lapsed monitoring and quantification of engineered bone-like tissue. Ann. Biomed. Eng. **35**: 1657–1667. doi:10.1007/s10439-007-9338-2

Jönsson, K. I. 2003. Causes and consequences of excess resistance in cryptobiotic metazoans. Physiol. Biochem. Zool. **76**: 429–435. doi:10.1086/377743

McGinnis, R. 2009. Rad pro X-ray device dose-rate calculator online. Massachusetts Institute of Technology.

Metscher, B. D. 2009. MicroCT for comparative morphology: Simple staining methods allow high-contrast 3D imaging of diverse non-mineralized animal tissues. BMC Physiol. **9**: 11. doi:10.1186/1472-6793-9-11

Parashar, V., S. Frankel, A. G. Lurie, and B. Rogina. 2008. The effects of age on radiation resistance and oxidative stress in adult *Drosophila melanogaster*. Radiat. Res. **169**: 707–711. doi:10.1667/RR1225.1

Pietrzak, B., and M. Slusarczyk. 2006. The fate of the ephippia–Daphnia dispersal in time and space. Pol. J. Ecol. **54**: 709–714. doi:10.1186/1472-6793-9-11

Pinceel, T., B. Vanschoenwinkel, and L. Brendonck. 2013a. Flexible dispersal dimorphism in zooplankton resting eggs: An example of repeated phenotypic coin flipping? Biol. J. Linn. Soc. **110**: 749–756. doi:10.1899/12.157.1 doi:10.1111/bij.12161

Pinceel, T., B. Vanschoenwinkel, J. Uten, and L. Brendonck. 2013b. Mechanistic and evolutionary aspects of light-induced dormancy termination in a temporary pond crustacean. Freshw. Sci. **32**: 517–524. doi:10.1899/12.157.1 doi:10.1899/12.157.1

Pinceel, T., L. Brendonck, and B. Vanschoenwinkel. 2016. Propagule size and shape may promote local wind dispersal in freshwater zooplankton—a wind tunnel experiment. Limnol. Oceanogr. **61**: 122–131. doi:10.1002/lno.10201

Rengle, A., and others. 2009. A dedicated two-channel phased-array receiver coil for high-resolution MRI of the rat knee cartilage at 7. IEEE Trans. Biomed. Eng. **56**: 2891–2897. doi:10.1109/TBME.2008.2006015

Schambach, S. J., S. Bag, L. Schilling, C. Groden, and M. A. Brockmann. 2010. Application of micro-CT in small animal imaging. Methods **50**: 2–13. doi:10.1016/j.ymeth.2009.08.007

Staedler, Y. M., D. Masson, and J. Schönenberger. 2013. Plant tissues in 3D via X-ray tomography: Simple contrasting methods allow high resolution imaging. Plos One **8**: e75295. doi:10.1371/journal.pone.0075295

Steppe, K., V. Cnudde, C. Girard, R. Lemeur, J. P. Cnudde, and P. Jacobs. 2004. Use of X-ray computed microtomography for non-invasive determination of wood anatomical characteristics. J. Struct. Biol. **148**: 11–21. doi:10.1016/j.jsb.2004.05.001

Timms, B. V., and S. Lindsay. 2011. Morphometrics of the resting eggs of the fairy shrimp 'Branchinella' in Australia (Anostraca: Thamnocephalidae). Proc. Linn. Soc. N. S. W. **133**: 52–68.

Tuytens, K., B. Vanschoenwinkel, A. Waterkeyn, and L. Brendonck. 2014. Predictions of climate change infer increased environmental harshness and altered connectivity in a cluster of temporary pools. Freshw. Biol. **59**: 955–968. doi:10.1111/fwb.12319

Vanschoenwinkel, B., M. T. Seaman, and L. Brendonck. 2010. Hatching phenology, life history and egg bank size of a fairy shrimp (Branchiopoda, Crustacea) in relation to the ephemerality of its habitat. Aquat. Ecol. **44**: 771–780. doi:10.1007/s10452-010-9315-y

Verboven, P., and others. 2013. Void space inside the developing seed of Brassica Napus and the modelling of its function. New Phytol. **199**: 936–947. doi:10.1111/nph.12342

Weston, A. E., H. E. Armer, and L. M. Collinson. 2010. Towards native-state imaging in biological context in the electron microscope. J. Chem. Biol. **3**: 101–112. doi:10.1007/s12154-009-0033-7

Yamauchi, D., and others. 2013. Micro-CT observations of the 3D distribution of calcium oxalate crystals in cotyledons during maturation and germination in Lotus

miyakojimae seeds. Microscopy **62**: 353–361. doi:10.1093/jmicro/dfs079

Zhou, L., and others. 2006. Linear energy transfer dependence of the effects of carbon ion beams on adventitious shoot regeneration from in vitro leaf explants of Saintpaulia Ionahta. Int. J. Radiat. Biol. **82**: 473–481. doi:10.1080/09553000600863080

## Acknowledgments

The authors would like to thank Nene Lefaible and Tim Sierens for assisting with the initial experiments for optimization of the μCT scanning settings and Alexander Vrijdaghs for conducting the SEM analysis. The authors are also grateful to the associate Editor and four anonymous reviewers for providing feedback which helped to improve the quality of the manuscript. T.P. is currently supported by a postdoctoral fellowship of the Research Foundation – Flanders (FWO, 12F0716N). This research benefitted from additional financial support from the Research Foundation – Flanders 3E090007 and 3E110799. The SkyScan 1172 high resolution micro-CT scanner, located at the facilities of Vrije Universiteit Brussel, was funded by the Hercules Foundation (UABR/11/004).

*Submitted 13 April 2016*
*Revised 12 July 2016*
*Accepted 26 July 2016*

*Associate editor: David G. Zawada*